J. Fluid Mech. (1988), *vol.* 194, *pp.* 457–478
Printed in Great Britain

Streaming motions in a bed of vibrationally fluidized dry granular material

By STUART B. SAVAGE
Department of Civil Engineering and Applied Mechanics, McGill University, Montreal, Canada

(Received 31 August 1983 and in revised form 21 January 1988)

Experimental and theoretical studies of vibration-induced flow and mixing of dry granular materials are described. Tests were performed on rounded polystyrene beads contained in a rectangular box having transparent front and back walls and a flexible, nominally horizontal bottom which could be driven at various frequencies and amplitudes. The amplitude of the bottom vibrations was a maximum at the centre and decreased towards the vertical sidewalls. Slow recirculating flows were observed; they had the form of two vortices in which the velocity was upwards at the vertical centreline and downwards along the vertical sidewalls. The streaming velocities were measured as a function of bed vibration frequency and displacement amplitude. An explanation proposed for the recirculating flows is that the vibrating base sends 'acoustic' waves upwards through the bed. These waves 'fluidize' the granular material but are in turn attenuated because of the dissipative nature of the collisions between the 'fluidized' particles. Thus the slow recirculating flows in the granular material are analogous to the more familiar 'acoustic streaming' in air. An approximate analysis of these streaming motions is developed by making use of a modification of the constitutive theory of Jenkins & Savage (1983). A number of simplifying assumptions are introduced to make the analysis tractable. The general flow patterns of the streaming motions are predicted, but the velocities are overestimated as a result of the simplifying assumptions. The analysis is restricted to a rather narrow range of conditions.

1. Introduction

Often, during the transportation, processing and handling of particulate solids, it can be beneficial to employ external sources of vibrational energy. For example, vibrations can be used to segregate different sizes and materials, to induce closer packing of the solids, and to 'fluidize' the granular material and thus improve its flow characteristics. Input of vibrational energy has also been suggested by a number of investigators as a possible means of mixing particulate solids. Kroll (1955) observed that slow circulatory motions occurred in a particle bed when the vessel containing the granular material was subjected to vertical sinusoidal vibrations. Takahashi, Suzuki & Tanaka (1968/9) and Suzuki, Takahashi & Tanaka (1968/9) investigated vibration-induced circulatory mixing in hopper-shaped vessels. More recently, Rátkai (1976) has measured the recirculating granular flows developed by vertical vibrations of a circular plate located in the central portion of the horizontal base of a 90 mm diameter cylindrical container. The circular plate induced upward spout-like velocities of the order of 1 cm/s above the plate in a 66 mm deep bed of 1 mm diameter plastic granules. The circulatory motions, which Rátkai termed the

'vibro-spouted' process, were most vigorous for vibration frequencies between 30 and 60 Hz.

Motivated more by scientific curiosity than by practical considerations of the above kind, Walker (1982) has made some amusing and surprising observations of the motions and circulatory patterns in vibrated dehydrated beverage powders (Nestea and Tang). Walker's experimental arrangement was based upon the classical demonstrations of Chladni that were performed in 1787. Chladni observed that sand grains sprinkled on a vibrating flat plate tend to collect along the nodal lines to form arrangements that are now known as Chladni patterns. He further observed that when the sand was replaced by a finer material such as lycopodium powder, the vibrations caused the powder to collect at the *antinodes*. The usual explanation, which has a sound theoretical basis, is that the plate vibrations generate 'acoustic streaming' in the air above the plate and these streaming motions in the air transport the fine light powder towards the antinodes.

Walker placed piles of Nestea and Tang powder upon a horizontal metal plate vibrated by a loudspeaker which in turn was driven by an audio oscillator. He was particularly interested in the circulation patterns developed *within* the powder itself. He found that the particles at the bottom of the pile moved towards the centre of the plate, rose upwards to the top of the pile, rolled down the sides and re-entered the pile at the bottom. The overall circulation pattern was similar to that in the 'vibro-spouted' beds described by Rátkai (1976). Similar observations were made much earlier by Faraday (1831) in connection with his investigations of Chladni patterns. Faraday's physical explanation for the circulatory motions in the powder pile was as follows. Near the peak of the pile's upward travel, the base of the pile loses contact with the plate, air rushes in the gap thus created and carries particles from the perimeter of the pile towards the centre. Walker (1982) found this explanation unsatisfactory and argued that particles at the base of the pile would be dragged in the opposite direction, from the centre to the rim, over the part of the cycle when the pile comes down towards the plate.

One possible approach to this problem would be a theoretical continuum, fluid-like description of the vibration-induced flow fields, based upon the solution of an appropriate set of governing equations of motion, but as yet this has not been attempted. In fact, not even a convincing physical argument to explain the cause of the circulatory flows has been previously suggested. The present paper describes experimental and theoretical studies intended to clarify the mechanics of the vibration-induced circulatory flows and mixing of dry granular material. This is attempted by directing attention to a specific boundary-value problem and choosing the flow geometry and boundary conditions so as to minimize the complexity of the theoretical analysis. The main objectives are to isolate the primary physical mechanisms that drive the circulations and to devise a simple analysis which is capable of predicting the essential features of the flow field and the order of magnitude of the velocities.

2. Exploratory experiments

As a preliminary to the analysis, some simple experiments were carried out under the author's direction by R. Kong and J. Lee as part of an undergraduate student project. The intent was to observe the circulation phenomenon in operation, to gain some appreciation of the collisional interactions that individual particles experience and the values of solids concentration that occur, and to determine typical

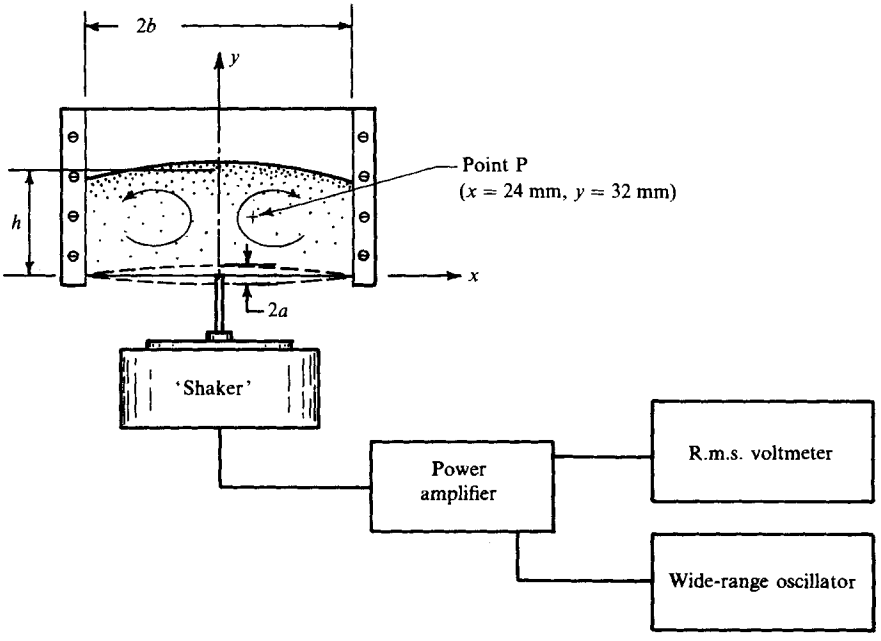

FIGURE 1. Schematic diagram of vibrating bed apparatus.

magnitudes for the circulation velocities and how they depend upon bottom-wall vibration frequency and amplitude. Since the main purpose was to acquire some broad physical impressions, the measurements were neither extensive nor very detailed.

2.1. *Apparatus and procedure*

A schematic diagram of the experimental apparatus is shown in figure 1. The granular material consisted of flattened, but roughly spherical, polystyrene particles having a specific gravity of 1.09 and diameters ranging between 0.8 and 2.0 mm. The particles were contained in a rectangular box having two vertical aluminium sidewalls spaced 180 mm apart, and vertical front and back walls spaced 19 mm apart and made of transparent plate glass to permit visual observations of the particle motions. The flexible, nominally horizontal sheet-metal bottom was attached at pinned supports to the vertical aluminium sidewalls and could be driven at various frequencies and amplitudes by a mechanical vibrator connected to an amplifier and oscillator. The amplitude of the base vibrations was spatially non-uniform, with a maximum at the vertical centreline and close to zero at the sidewalls.

By mixing in a small quantity of black particles with the mass of white polystyrene beads it was possible to distinguish clearly the streamline patterns. Velocities were determined by measuring the lengths of streamlines made on film by these particles during time exposures taken by a 35 mm still camera. Figure 2 is a typical (long) time exposure showing the two recirculating cells that developed. The particles moved upward along the centreline and downward near the sidewalls. For the experimental results presented here, the flow patterns were reasonably two-dimensional; however, there were instances in which strong three-dimensional streamline patterns were observed. Experiments were performed during the winter months under conditions where the humidity was very low. It was found that when the beads were vibrated for 5–10 min, a significant electrostatic charge would develop. When this happened,

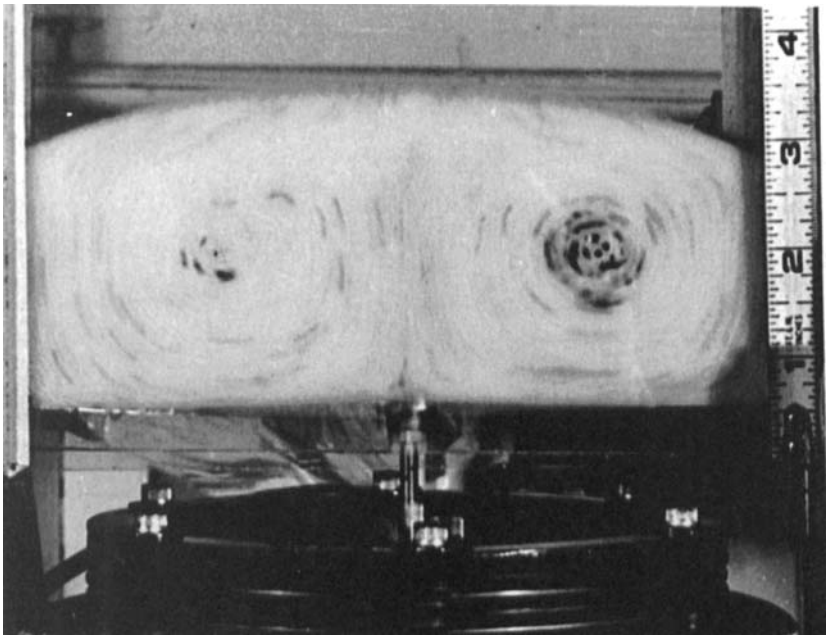

FIGURE 2. 'Long' time exposure of vibrated granular bed. Streaks made by black beads indicate circulatory streaming motions.

particles were attracted to each other and to the glass sidewalls, and the recirculating motions were retarded. These difficulties were significantly reduced by spraying the particles prior to each test with antistatic liquid of the kind used to prevent collection of dust on phonograph records.

Series of tests were performed to investigate the effects of the amplitude and frequency of the base vibrations on the strength of the recirculating motions. Rather than map out the whole velocity field for each test, a representative velocity V_P was determined from streamline measurements in the region of a point P located 32 mm above the bed level and 24 mm from the vertical centreline as shown in figure 1. In a given set of tests at a fixed vibration frequency, the velocities at the point P were measured for series of values of base centreline vibration displacement amplitudes a. The data for various frequencies were cross-plotted in terms of velocity versus frequency for various values of a, as shown in figure 3.

One of the referees of an earlier version of the present paper drew attention to Gutman's (1976) work which studied the fluidization of powder by vibration of its rigid cylindrical container. Temporal variations of the interstitial fluid pressure occurred and fluidization was attributed to the net upward force generated because the pressure variations were not in phase with the particle motion. Such interstitial fluid effects were not thought to be operative in the present tests since the particles used here were more than an order of magnitude larger than those used by Gutman. Furthermore, an air gap existed between the sidewalls and the vibrating bottom in the present tests, but no leakage could occur through the walls of Gutman's rigid container.

Nevertheless, as a matter of interest, a second set of tests was performed to compare circulation velocities generated when the solid vibrating plate was replaced by one that was perforated with circular holes of 0.794 mm ($\frac{1}{32}$ in.) spaced

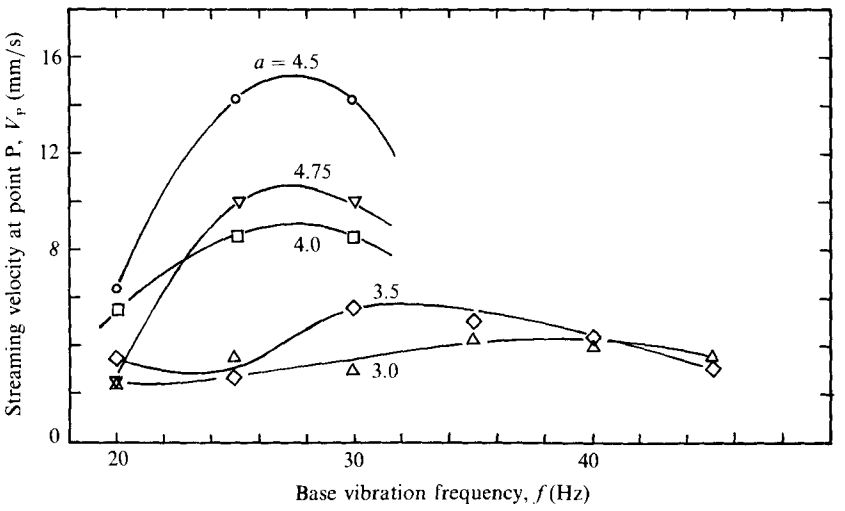

FIGURE 3. Experimentally determined magnitude of streaming velocity at point P as a function of bed vibration frequency and displacement amplitude.

approximately 3 mm between centres. The idea was to permit ready leakage of air through the bottom plate and prevent the development of significant interstitial fluid pressure variations. Some differences between the test results obtained with the solid vibrating bottom and the perforated one were observed, but it is most likely that these differences were due to the differences in effective wall roughness caused by the perforations rather than by interstitial fluid effects. In summary it was found that

(i) At lower displacement amplitudes a of 2.5–3 mm the solid plate generated about 30% higher circulation velocities than the perforated plate in the frequency range of 15–45 Hz.

(ii) For a between 3.5 and 4.5 mm the velocities were similar in magnitude except at frequencies greater than 30 Hz where the circulation velocities were lower for the perforated plate than for the solid plate.

(ii) For $a = 5$ mm, again the velocities were similar except for frequencies greater than 25 Hz where the perforated plate generated *higher* circulation velocities.

Two or three observations were taken for each set of test conditions to obtain the streaming-velocity data points. To give some idea of the reproducibility of results we note that an average of the differences between successive tests for the same conditions was 11.4%, but differences of up to 35% were observed.

2.2. *Results and a physical interpretation*

Each of the curves for constant a presented in figure 3 shows the same trend; the mean flow velocity at the point P increases with base vibration frequency f, reaches a maximum, and then decreases with further increase in f. With increase in amplitude a, the circulatory velocities initially increase and the peak in velocity at a constant value of a shifts to lower frequencies. When the base vibration amplitude a reaches a certain value, the circulatory velocities peak and further increases in amplitude reduce the circulation velocities. The general trends in these two-dimensional flow experiments are much the same as those observed by Rátkai (1976) in his axisymmetric apparatus. The two apparatuses were of roughly the same overall dimension and, as might be expected, the magnitudes of the circulation

velocities, and the ranges of operative bed frequencies and amplitudes were similar.

A physical explanation of the above results is now presented prior to the detailed analysis of the circulatory flow field. While this physical proposal may be accepted as natural and perhaps obvious by the reader, the task of identifying it as a likely flow mechanism was for the present writer assiduous. In fact, it was preceded by numerous attempts to pose the appropriate boundary-value problem by isolating essential mechanisms and specifying boundary conditions, all of which initially seemed plausible and reasonable, but which were found to be entirely unsatisfactory when the predictions of the circulatory velocities were compared with the experimental values. In most of these attempts, the correct senses of the recirculating motions were not even predicted.

The present notion is that the granular material is in a state similar to that described by the kinetic theories of granular flows (Savage 1983*a*, 1984) in which the individual particles are in continuous agitation as a result of collisions with near neighbours. Because of the particles' inelasticity and friction the collisions are dissipative and energy must flow from the bulk motion in order to maintain the particles' collisional velocity fluctuations. In some previous granular flow investigations, the bulk motion consisted of steady shear flows (see, for example, Shen & Ackermann 1982; Campbell & Brennen 1983, 1985; Haff 1983; Jenkins & Savage 1983; Savage 1983*a*; Lun *et al.* 1984; Jenkins & Richman 1985).

Here we consider the granular material as a compressible 'fluid' in the continuum context and regard the propagation of waves (analogous to acoustic waves) through it as the primary flow which maintains the particle velocity fluctuations or what is termed the 'granular temperature'. Thus the vibrating base sends waves upwards through the granular material. Because of the energy dissipation, the wave is attenuated as it propagates upward. The wave attenuation gives rise to a *mean force* on a 'fluid' element which results from the differences between the values of the Reynold's stresses acting on opposite sides of the element (Lighthill 1978, §4.7). Since the displacement amplitude of the bed vibrations is spatially non-uniform (largest at the centreline and smallest near the sidewalls), the amplitude of the waves originating at the bed is also spatially non-uniform. Hence the wave attenuation and thus the *mean force* field are non-uniform. The mean force field is strongest near the centreline; this generates two slow recirculating vortices in which material moves upwards along the vertical centreline and downwards along the sidewalls. Therefore, it is proposed that the circulatory motions are simply another example of 'acoustic streaming', but, in the present instance, streaming that occurs in a granular medium.

One would expect that as the displacement amplitude and frequency of the bed vibrations are increased from low values, the strength of the recirculating motions would increase. Such behaviour is evident in figure 3. In the interior of the mass of granular material a significant contribution to the pressure is due to collisions between particles, much like the pressure in a gas at the molecular level. The granular material thus behaves as a compressible fluid and particles can maintain collisional contact with the vibrating bed over the *complete cycle* of its travel as long as the accelerations and velocities of the vibrating bed are not too large. If the bed vibrations have too high a frequency or amplitude, so as to exceed some critical bed acceleration or velocity, the bed will lose collisional contact with the granular material over part of the cycle. During the motion upward from its lowermost position the vibrating bottom slams into the granular material and chattering

results. Thus, as the bed accelerations are increased above a critical value, the bed vibrations are less effective in inducing pressure waves through the material and the slow streaming recirculation velocities are reduced. This explains the maxima in the data shown in figure 3.

3. Governing equations

3.1. *Continuum equations for granular flow*

Jenkins & Savage (1983) (see also Savage 1983*a*, *b*, 1984, for experimental verification and further discussion of the theory) have developed a theory for the flow of idealized granular materials consisting of smooth but inelastic, identical spherical particles undergoing binary collisions. Although more detailed and complete analyses have recently been performed, for example by Lun *et al.* (1984) and Jenkins & Richman (1985), the simpler analysis of Jenkins & Savage will suffice for the present purposes. They supposed that, as a result of either some imposed mean shear flow or some input of vibrational energy as in the present case, particles continually collide with each other and dissipate energy as a consequence of the particles' inelasticity. Associated with these collisional translational velocity fluctuations we can define a *translational granular temperature* T, which is related to the fluctuation specific kinetic energy as follows:

$$\tfrac{3}{2}T = \tfrac{1}{2}\langle C^2\rangle, \tag{1}$$

where $\boldsymbol{C} = \boldsymbol{c} - \boldsymbol{u}$, $\boldsymbol{c}$ is the instantaneous velocity of an individual particle and $\boldsymbol{u} = \langle \boldsymbol{c}\rangle$ is the bulk velocity. The conservation equations for mass, momentum and fluctuation-specific kinetic energy have the familiar forms

$$\frac{\mathrm{d}\rho}{\mathrm{d}t} = -\rho\boldsymbol{\nabla}\cdot\boldsymbol{u}, \tag{2}$$

$$\rho\frac{\mathrm{d}\boldsymbol{u}}{\mathrm{d}t} = \rho\boldsymbol{g} - \boldsymbol{\nabla}\cdot\boldsymbol{p}, \tag{3}$$

$$\tfrac{3}{2}\rho\frac{\mathrm{d}T}{\mathrm{d}t} = -\boldsymbol{p}:\boldsymbol{\nabla u} - \boldsymbol{\nabla}\cdot\boldsymbol{q} - \gamma_{\mathrm{c}}, \tag{4}$$

where $\rho = mn = \nu\rho_{\mathrm{p}}$ is the bulk mass density, m and ρ_{p} are respectively the mass and mass density of individual particles, n is the number density of particles, ν is the solids fraction (volume of solids per unit volume), $\boldsymbol{p}$ is the pressure tensor composed of a kinetic part $\boldsymbol{p}_{\mathrm{k}} = \rho\langle\boldsymbol{CC}\rangle$ and a collisional part $\boldsymbol{p}_{\mathrm{c}}$, $\boldsymbol{q}$ is the flux of fluctuation energy composed of a kinetic part $\boldsymbol{q}_{\mathrm{k}} = \frac{1}{2}\rho\langle\boldsymbol{CC}^2\rangle$ and a collisional part $\boldsymbol{q}_{\mathrm{c}}$, γ_{c} is the collisional rate of dissipation per unit volume, $\boldsymbol{g}$ is the gravitational acceleration and t is time. For moderately large concentrations it is permissible to neglect the kinetic contributions in comparison with the collisional ones, and hence we assume $\boldsymbol{p}_{\mathrm{k}} \ll \boldsymbol{p}_{\mathrm{c}}$ and $\boldsymbol{q}_{\mathrm{k}} \ll \boldsymbol{q}_{\mathrm{c}}$. The constitutive equations for stress, energy flux and dissipation rates were found to be

$$\boldsymbol{p} \approx \boldsymbol{p}_{\mathrm{c}} = \left[\frac{\kappa}{\sigma}(\pi T)^{\frac{1}{2}} - \frac{\kappa}{5}(2+\alpha)\,\mathrm{tr}\,\boldsymbol{D}\right]\boldsymbol{I} - \frac{2\kappa}{5}(2+\alpha)\,\boldsymbol{D}, \tag{5}$$

$$\boldsymbol{q} = \boldsymbol{q}_{\mathrm{c}} = -\kappa\boldsymbol{\nabla}T, \tag{6}$$

$$\gamma_{\mathrm{c}} = \frac{6(1-e)\kappa}{\sigma^2}\left[T - \left(\frac{\pi}{4}+\frac{\alpha}{3}\right)\sigma\left(\frac{T}{\pi}\right)^{\frac{1}{2}}\mathrm{tr}\,\boldsymbol{D}\right], \tag{7}$$

where
$$\kappa = 2\nu^2(1+e)\,g_0\rho_p\sigma(T/\pi)^{\frac{1}{2}}, \tag{8}$$
$$\boldsymbol{D} = \tfrac{1}{2}(u_{i,j}+u_{j,i}), \tag{9}$$

σ is the particle diameter, e is the coefficient of restitution, $g_0(\nu)$ is the radial distribution function at contact and α is the numerical coefficient which we can take to be unity (Savage 1983*a*).

Following Savage & Jeffrey (1981), Jenkins & Savage (1983) used the radial distribution function $g_0(\nu)$ that was proposed by Carnahan & Starling (1969) on the basis of their numerical simulation carried out during 'equilibrium' (no shear):

$$g_0(\nu) = \frac{1}{1-\nu}+\frac{3\nu}{2(1-\nu)^2}+\frac{\nu^2}{2(1-\nu)^3} = \frac{(2-\nu)}{2(1-\nu)^3}.$$

A recent comparison in Lun *et al.* (1984) of the Jenkins & Savage (1983) theory with shear-cell experiments of Savage & Sayed (1984) suggests that the predictions for stresses are too low at high ν, but that most of the general trends of this theory are correct. It is proposed here that we replace the above expression for $g_0(\nu)$ by the simple one that is implicit in the work of Bagnold (1954) and was given later by Ogawa, Umemura & Oshima (1980):

$$g_0(\nu) = [1-(\nu/\nu_M)^{\frac{1}{3}}]^{-1}. \tag{10}$$

For a regular packing of equal spheres the maximum solids fraction $\nu_M = \pi/(3\sqrt{2}) = 0.7405$, for a random packing $\nu_M \approx 0.64$, but an appropriate value for ν_M when g_0 is used in the kinetic flow theory may be somewhat less than 0.64. If we take ν_M to be 0.7405, the numerical values given by (10) are close to those given by the expression of Carnahan & Starling; but, if we take $\nu_M = 0.64$ and use (10) for $g_0(\nu)$ in the Jenkins & Savage (1983) theory, then the predictions for the stresses are closer to the experimental results for what are probably realistic values of the coefficient of restitution. Hence, in the subsequent analysis we shall use (10) with $\nu_M = 0.64$.

The theory of Jenkins & Savage (1983) described above was developed for moderate concentrations, high enough that the kinetic contributions can be neglected, but low enough that the assumption of binary collisions is still valid. At higher concentrations the assumption of binary collisions breaks down. Collisions cannot be regarded as instantaneous, and ternary and higher-order collisions as well as enduring contacts between particles will occur. As a result of dry Coulomb friction and particle overriding during enduring contacts, rate-independent stresses are developed in addition to the collisional rate-dependent stresses.

It is far from clear how to devise a rational theory which includes these rate-independent effects, but Savage (1983*b*) has suggested a simple *ad hoc* approach to account for them in a crude way. The total stress tensor was assumed to be composed of the sum of a quasi-static or rate-independent part $\boldsymbol{p}_s$ and a collisional momentum flux part $\boldsymbol{p}_c$ given by (5), thus
$$\boldsymbol{p} \approx \boldsymbol{p}_s + \boldsymbol{p}_c. \tag{11}$$

The kinetic contribution arising from translation of particles across shear planes was again neglected. The rate-independent part $\boldsymbol{p}_s$ was assumed to be of the form

$$\boldsymbol{p}_s = p_{s_0}\boldsymbol{I} - p_{s_0}\sin\varphi\frac{\boldsymbol{D}}{(\frac{1}{2}\operatorname{tr}\boldsymbol{DD})^{\frac{1}{2}}}, \tag{12}$$

where $\operatorname{tr}(\boldsymbol{DD}) = D_{im}D_{mi}$, p_{s_0} is the mean 'quasi-static' normal stress, and φ is the

quasi-static friction angle which in general might be a function of concentration ν and the granular temperature T. The total stress $\boldsymbol{p}$ must satisfy the linear momentum equation (3). It was assumed that the granular temperature was governed by the collisional-fluctuation-energy equation

$$\tfrac{3}{2}\rho\frac{\mathrm{d}T}{\mathrm{d}t} = -\boldsymbol{p}_{\mathrm{c}}:\boldsymbol{\nabla u} - \boldsymbol{\nabla}\cdot\boldsymbol{q}_{\mathrm{c}} - \gamma_{\mathrm{c}}. \tag{13}$$

In addition to the collisional dissipation γ_{c}, which appears in (13), we note that in general there is an additional dissipation term γ_{s} associated with the stress work $\boldsymbol{p}_{\mathrm{s}}:\boldsymbol{\nabla u}$, the evolution of the ordinary temperature and heat conduction.

Furthermore, in the present paper it is assumed that, because of the presence of the vibrations, the quasi-static friction angle φ tends to vanish. With the above assumptions the stress tensor (11) after taking $\alpha = 1$, simplifies to

$$\boldsymbol{p} = \boldsymbol{p}_{\mathrm{s}} + \boldsymbol{p}_{\mathrm{c}} = \left[p_{\mathrm{s}_0} + \frac{\kappa}{\sigma}(\pi T)^{\frac{1}{2}} - \frac{3\kappa}{5}\operatorname{tr}\boldsymbol{D}\right]\boldsymbol{I} - \frac{6\kappa}{5}\boldsymbol{D}. \tag{14}$$

The above constitutive equations are admittedly oversimplified and *ad hoc* in certain respects, but at the present time we have little else to use.

3.2. *'Sound' speed*

In the analysis developed in §4 we require the speed of propagation of infinitesimal waves through the granular medium consisting of particles that are excited and continuously colliding. To get a rough estimate of this 'sound' speed we follow the analysis given in Chapman & Cowling (1960, pp. 396–398) dealing with damping of sound waves in a gas. We note that Haff (1983) has given a brief and somewhat different discussion of the sound speed in a granular medium.

Neglecting the dissipation γ_{c} and the flux of fluctuation energy $\boldsymbol{g}_{\mathrm{c}}$, the energy equation (13) reduces to

$$\tfrac{3}{2}\rho\frac{\mathrm{d}T}{\mathrm{d}t} = -\boldsymbol{p}_{\mathrm{c}}:\boldsymbol{\nabla u}. \tag{15}$$

If we neglect terms analogous to the usual viscosities then the collisional stress tensor is

$$\boldsymbol{p}_{\mathrm{c}} = p_0\boldsymbol{I}, \tag{16}$$

where

$$p_0 = 2(1+e)\,\nu g_0(\nu)\rho T = \Gamma(\nu)\rho T, \tag{17}$$

and hence

$$\boldsymbol{p}_{\mathrm{c}}:\boldsymbol{\nabla u} = p_0\boldsymbol{\nabla}\cdot\boldsymbol{u}. \tag{18}$$

Using the mass-conservation equation (2) and (18) in (15) yields the 'sound speed'

$$c_0 = \left(\frac{\partial p}{\partial \rho}\right)^{\frac{1}{2}} = \left[\left(1 + \tfrac{2}{3}\Gamma + \frac{\nu}{\Gamma}\frac{\mathrm{d}\Gamma}{\mathrm{d}\nu}\right)\Gamma T\right]^{\frac{1}{2}}. \tag{19}$$

The ratio $c_0/T^{\frac{1}{2}}$ versus ν is shown in figure 4. Curves are shown for different values of e although we realize that it is somewhat inconsistent to do so since we have neglected terms like the dissipation γ_{c} in the determination of (19).

Since signals propagate as a result of particle collisions, we might expect that at very low concentrations, $c_0 \approx \langle C^2\rangle^{\frac{1}{2}} = (3T)^{\frac{1}{2}}$. At higher concentrations, we can roughly estimate c_0 as follows. Define s as the mean free separation distance between particles, so that $(s+\sigma)$ is the mean distance between centres. We may express s in

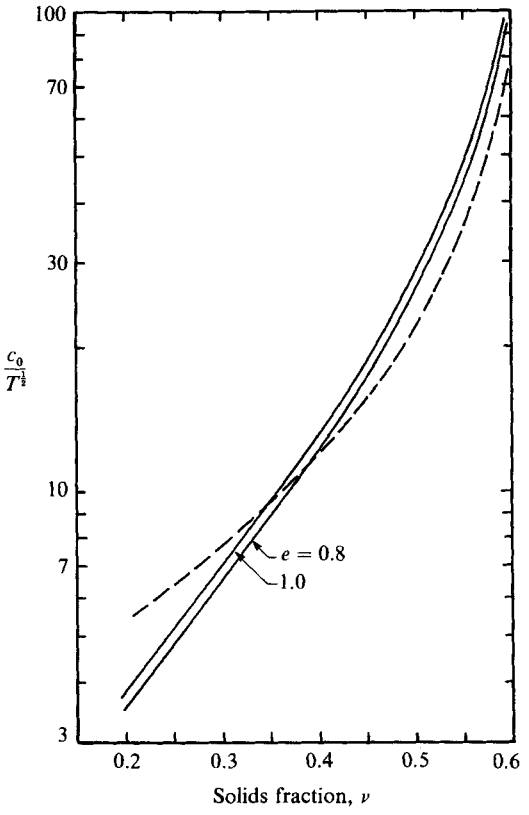

FIGURE 4. Variation of $c_0/T^{\frac{1}{2}}$ with solids fraction ν: ——, equation (19); – – –, equation (21).

terms of the concentration ν and the maximum possible concentration for a regular dense packing ν_M (Bagnold 1954). Thus the linear concentration is

$$\lambda = \frac{\sigma}{s} = \left[\left(\frac{\nu_M}{\nu}\right)^{\frac{1}{3}} - 1\right]^{-1}. \tag{20}$$

For a signal to propagate a distance $(\sigma + s)$, a particle moving at the r.m.s. fluctuation velocity $\langle C^2\rangle^{\frac{1}{2}}$ need only traverse a distance s. A rough estimate of c_0 is thus

$$c_0 = \left(\frac{\sigma + s}{s}\right)\langle C^2\rangle^{\frac{1}{2}} = (\lambda + 1)(3T)^{\frac{1}{2}}. \tag{21}$$

Equation (21) is also shown on figure 4; it yields values for c_0 somewhat lower than those given by (19) for the range of ν of interest here.

3.3. *Continuum mean flow and fluctuation equations*

The mean flow and fluctuation equations are now obtained from the conservation equations for mass, momentum and fluctuation-specific kinetic energy (2), (3) and (4). It is important to realize that in this section the averaging is carried out over a coarser scale than that used to derive (2)–(4). The flow velocity fluctuations dealt with in this section should not be confused with particle velocity fluctuations $\boldsymbol{C}$. We follow the method of mass-weighted averaging which is commonly used in studies of compressible flow turbulence (Cebeci & Smith 1974). Note that whereas in turbulent

shear flow problems the fluctuations are often rather smaller than the mean flow properties, in the present problem the mean flow velocities corresponding to the streaming flow will be considered small compared with the velocity fluctuations associated with the wave motions generated by the vibrating base.

Write the velocity components and density in terms of mean and fluctuating parts:

$$u_i = \tilde{u}_i + u_i', \tag{22}$$

$$\rho = \bar{\rho} + \rho'', \tag{23}$$

where

$$\tilde{u}_i = \overline{\rho u_i}/\bar{\rho} \tag{24}$$

is a mass-weighted mean velocity component and the overbar denotes the usual mean.

Writing the expression for $\overline{\rho u_i}$ in terms of the definitions (22)–(24) we find

$$\overline{\rho u_i'} = 0. \tag{25}$$

Similarly, we write the 'granular temperature' in terms of mean and fluctuating parts:

$$T = \tilde{T} + T', \tag{26}$$

where

$$\tilde{T} = \overline{\rho T}/\bar{\rho} \tag{27}$$

is the mass-weighted mean granular temperature and

$$\overline{\rho T'} = 0. \tag{28}$$

The conservation equations (2)–(4) may then be expressed as

$$\frac{\partial}{\partial t}(\bar{\rho} + \rho'') + \frac{\partial}{\partial x_j}(\rho \tilde{u}_j + \rho u_j') = 0, \tag{29}$$

$$\frac{\partial}{\partial t}(\rho \tilde{u}_i + \rho u_i') + \frac{\partial}{\partial x_j}[\rho \tilde{u}_i \tilde{u}_j + \rho \tilde{u}_i u_j' + \rho u_i' \tilde{u}_j + \rho u_i' u_j'] = \rho g_i - \frac{\partial p_{ij}}{\partial x_j}, \tag{30}$$

and

$$\frac{3}{2}\left[\frac{\partial}{\partial t}(\rho \tilde{T} + \rho T') + \frac{\partial}{\partial x_j}(\rho \tilde{T} \tilde{u}_j + \rho T' \tilde{u}_j + \rho \tilde{T} u_j' + \rho T' u_j')\right] = -p_{ij}\frac{\partial u_i}{\partial x_j} - \frac{\partial q_i}{\partial x_j} - \gamma_c. \tag{31}$$

Taking the means of these equations yields

$$\frac{\partial}{\partial x_j}(\bar{\rho} \tilde{u}_j) = 0, \tag{32}$$

$$\frac{\partial}{\partial t}(\bar{\rho} \tilde{u}_i) + \frac{\partial}{\partial x_j}(\bar{\rho} \tilde{u}_i \tilde{u}_j) = \bar{\rho} g_i - \frac{\partial \bar{p}_{ij}}{\partial x_j} - \frac{\partial}{\partial x_j}(\overline{\rho u_i' u_j'}), \tag{33}$$

$$\frac{3}{2}\left[\frac{\partial}{\partial t}(\bar{\rho} \tilde{T}) + \frac{\partial}{\partial x_j}(\bar{\rho} \tilde{T} \tilde{u}_j)\right] = -\frac{\partial}{\partial x_j}(\overline{\rho T' u_j'}) - \frac{\partial \bar{q}_i}{\partial x_j} - \overline{\gamma_c} - \overline{p_{ij}\frac{\partial u_i}{\partial x_j}}, \tag{34}$$

where the stress has been separated into a mean and fluctuating part:

$$p_{ij} = \bar{p}_{ij} + p_{ij}''. \tag{35}$$

3.4. *A rough order-of-magnitude estimate of the streaming velocities based upon the proposed streaming mechanism*

Prior to performing the detailed analysis of §4 we shall present some rough computations to estimate the order of magnitude of the streaming velocities. This

section can be regarded as a more detailed and quantitative elaboration of §2.2 which presented a physical description of the proposed mechanism responsible for the streaming motions. The purpose is to obtain some quantitative predictions of the streaming velocities in a simple and direct way for the reader who may not wish to read in detail the analysis of §4.

We consider the circulatory motion associated with the gyre in the right-hand half of the vibrating granular material (see figure 1). The mass of fluidized particles, when sheared, will exhibit an effective shear viscosity which we assume can be determined from the Jenkins–Savage theory. From (14) this viscosity is seen to be $3\kappa/5$, where κ is given by (8). In the steady state, the resulting magnitudes of the streaming velocities in the gyre are such that the rate of 'viscous' dissipation is just balanced by the rate at which work is done by the distributed force resulting from the attenuation of the waves propagating upwards from the bed. This condition can be used as a very simple way to estimate the magnitude of the circulation velocities.

For sinusoidal waves the Reynolds stress at the bed is $\frac{1}{2}\bar{\rho}v_b^2$ where $v_b(x)$ is the magnitude of vertical velocity of the vibrating bottom. Note that the velocity $v_b(x)$ varies with position since the displacement amplitude of the vibrating bottom varies, having a maximum value a at the centreline and decreasing towards the vertical sidewalls. Assuming that there is a 50% attenuation in Reynolds stresses over the complete depth, the (depth-averaged) distributed force per unit volume due to these Reynolds stress is $(1/h)(\frac{1}{4}\bar{\rho}v_b^2)$.

Particles move in a clockwise direction in the right-hand gyre, i.e. upward along the vertical centreline and downward along the right-hand sidewall, with an approximate speed that we shall call v_e. The particles also move towards the right along the top surface and to the left along the bottom with an approximate speed of u_e. From the conservation of mass within the recirculating gyre we see that roughly

$$u_e h = v_e b.$$

Positive work is done by the distributed (upward) force over the half of the gyre where the particles have an upward streaming velocity component. Assume that over the portion of the vibrating bottom directly below this region the average value of v_b^2 is $\frac{1}{2}a^2\omega^2$, where ω is the radian frequency of the bottom vibrations. Multiplying the resulting distributed force per unit volume by the average upward streaming velocity over the associated half of the gyre (assumed to be $\frac{1}{3}v_e$) and by the area itself ($\frac{1}{2}bh$) yields the rate at which work is done by the distributed force (per unit thickness of the granular bed):

$$\frac{\bar{\rho}a^2\omega^2}{8h}(\tfrac{1}{3}v_e)(\tfrac{1}{2}bh).$$

We neglect the (negative) contribution from the half of the gyre where the streaming velocities have a downward component. These downward velocities are largest in the region next to the right-hand sidewall, but there the Reynolds stresses are smallest because the bottom displacements are small. Thus, the work contribution from this half of the gyre is only a fraction of the work done in the region where the streaming velocities have an upward component.

Using the value of $3\kappa/5$ from the Jenkins–Savage theory for the effective viscosity we can write the 'viscous' dissipation rate per unit volume for the assumed incompressible material as

$$\tfrac{6}{5}\kappa(D_{ij}D_{ij}).$$

We approximate the value of D_{ij} in the gyre as $\frac{1}{2}[\frac{1}{2}(2u_e/h + 2v_e/b)] = \frac{1}{2}v_e(1+b^2/h^2)/b$ (assuming linear variations of velocity from the centre of the gyre and

using $u_e = v_e(b/h)$). Now multiply the dissipation rate per unit volume by the area of the gyre bh to obtain the dissipation rate per unit thickness of the granular bed as

$$\tfrac{3}{10}\kappa v_e^2 \left(\frac{h}{b}\right)\left(1+\frac{b^2}{h^2}\right)^2.$$

Now by using (8) for κ and setting the rate at which work is done by the distributed force equal to the rate of dissipation we can obtain an expression for the streaming velocity component v_e:

$$v_e = \frac{5a^2\omega^2 b^2(\pi/T)^{\frac{1}{2}}}{144\nu(1+e)\,g_0\,\sigma h(1+b^2/h^2)^2}.$$

The most difficult thing to estimate without the benefit of detailed microscopic energy considerations is the granular temperature T over the main part of the bed. From (1) we see that T is defined to be a third of the mean square of the particle velocity fluctuations. If the particles exactly followed the motion of the sinusoidal bed vibrations then the maximum value of $T^{\frac{1}{2}}$ at the centreline (left-hand edge of the gyre) would equal $(a\omega)/\sqrt{6}$. The displacement amplitude of the particle fluctuations in the main part of the bed was observed to be quite a bit smaller than the centreline amplitude of the bed vibrations, so this probably considerably overestimates the granular temperature over the major part of the bed. If, on the other hand, particles bounce back and forth across the mean separation distance between particles s with a frequency $f = \omega/2\pi$, then $T^{\frac{1}{2}} = (s\omega/\pi)/\sqrt{6}$, a considerably smaller value. As a very rough guess for the choice of an appropriate value of T, we reduce the first estimate to $T^{\frac{1}{2}} = (a\omega)/6$ to account for fluctuations of an amplitude smaller than a over the main part of the gyre. (We note that the more detailed energy considerations of §4.1 give a result that can be expressed very roughly for the present experiments as $T^{\frac{1}{2}} \approx (as)^{\frac{1}{2}}\omega$.)

Let us now substitute for the variables in the above equation for v_e numerical values corresponding to the experiments described in §2. Thus take $h = 62$ mm, $b = 90$ mm, the average particle diameter as $\sigma = \frac{1}{2}(0.8+2.0) = 1.4$ mm, assume that the average solids fraction $\nu = 0.58$, and determine g_0 from (10). These are the same values that will be used later in predictions based upon the more detailed theory of §5. If we choose, for example, $a = 3$ mm and a bed vibration frequency $f = 30$ Hz we find that the streaming velocity $v_e = 61$ mm/s. Using $T = as\omega^2$ gives a streaming velocity $v_e = 81$ mm/s. These values are of the same order as that predicted by the more detailed analysis of §4 (see figure 6). All are considerably larger than the experimental values because of the neglect of friction on the sidewalls of the container (particularly the walls of area bh) and the neglect of the quasi-static contribution to the shear stresses in the interior of the material as discussed in §5.

4. Analysis

Solution of (29)–(34) and the associated constitutive equations for p_{ij}, q_j and γ_c for the present problem is formidable and may be possible only through the use of numerical methods. The purpose of the present paper is merely to explore the mechanics that govern the development of the vibration-induced circulating flow patterns. Accordingly we shall choose a particular geometry and make linearizations and other assumptions to permit a simple approximate solution which can be expressed in analytical form.

Consider two-dimensional motions in the x, y (x_1, x_2)-plane. Assume that the mean

depth of granular material h is small compared with the half-width b of the rectangular container (figure 1) and that the amplitude of the base vibration is a maximum in the centre of the container at $x = 0$, and that its variation with x is not large; hence $\partial/\partial x \ll \partial/\partial y$. It is assumed that the steady mass-weighted mean velocity is small compared with the velocity fluctuations associated with the wave motions, but that the other fluctuating quantities such as density, granular temperature and stress are small compared with the respective mean values, i.e.

$$\tilde{u}_i \ll u_i', \tag{36}$$

but

$$\rho'' \ll \bar{\rho}, \tag{37}$$

$$T' \ll \tilde{T}, \quad \text{etc.} \tag{38}$$

With these assumptions the mean linear momentum equation (33) is approximated by

$$0 = \bar{\rho} g_i - \frac{\partial \bar{p}_{ij}}{\partial x_j} - \frac{\partial}{\partial x_j}(\overline{\rho u_i' u_j'}), \tag{39}$$

and the momentum equation (30) by

$$\frac{\partial}{\partial t}(\bar{\rho} u_i') + \frac{\partial}{\partial x_j}[\bar{\rho} u_i' u_j'] = \bar{\rho} g_i - \frac{\partial p_{ij}}{\partial x_j}. \tag{40}$$

4.1. *The primary wave motions*

Subtracting (39) from (40) and assuming that $(\partial/\partial x_j)[\bar{\rho}(u_i' u_j' - \overline{u_i' u_j'})]$ is small compared with the other terms, and that $\bar{\rho} \approx \rho_0 = \text{const}$, yields the linearized momentum equation

$$\rho_0 \frac{\partial u_i'}{\partial t} = -\frac{\partial p_{ij}''}{\partial x_j}. \tag{41}$$

The dominant terms of the y-equation of (41) are

$$\rho_0 \frac{\partial v'}{\partial t} = -\frac{\partial p_{yy}''}{\partial x_j}, \tag{42}$$

where from (14) p_{yy}'' is written as

$$p_{yy}'' = p'' - \frac{3\kappa}{5}\frac{\partial v'}{\partial y} - \frac{6\kappa}{5}\frac{\partial v'}{\partial y}. \tag{43}$$

For simplicity we assume that κ is constant; in general this would be quite a crude approximation, but for the present case it may not be too extreme since near the vibrating base where the granular temperature is high, $\nu^2 g_0(\nu)$ is probably low whereas nearer the free surface the opposite is likely to be true (see (8)). Substituting (43) in (42) yields

$$\rho_0 \frac{\partial v'}{\partial t} = -c_0^2 \frac{\partial \rho''}{\partial y} + \frac{9\kappa}{5}\frac{\partial^2 v'}{\partial y^2}, \tag{44}$$

where

$$c_0^2 = \frac{\partial p''}{\partial \rho}, \tag{45}$$

and c_0 is the 'sound speed' defined by (19).

In a similar way, from the conservation-of-mass equations (29) and (32) we obtain

$$\frac{\partial \rho''}{\partial t} = -\rho_0 \frac{\partial v'}{\partial y}. \tag{46}$$

Eliminating ρ'' from (44) and (46) yields the damped wave equation for v' (Lighthill 1978, pp. 76–80)

$$\frac{\partial^2 v'}{\partial t^2} = c_0^2 \frac{\partial^2 v'}{\partial y^2} + \frac{9\kappa}{5\rho_0} \frac{\partial^3 v'}{\partial t \partial y^2}. \tag{47}$$

For *small attenuation* (47) has solutions of the form

$$v' = v_b(x) \cos(ky - \omega t)\, e^{-\delta y}, \tag{48}$$

where

$$k = \frac{\omega}{c_0}, \quad \delta = \frac{9\kappa\omega^2}{10\rho_0 c_0^3}, \tag{49}$$

$v_b(x)$ is the vertical velocity at the base and is a slowly varying function of x, and ω and k are the radian frequency and wavenumber of the longitudinal waves travelling upward through the granular material.

To first order for small damping, the density fluctuation

$$\rho'' = -\frac{\rho_0}{c_0} v'. \tag{50}$$

For a steady streaming flow, the dominant terms in the energy equation (34) after making use of (14) are found to be

$$\frac{\partial^2 \tilde{T}}{\partial x_j \partial x_j} - \frac{6(1-e)}{\sigma^2}\tilde{T} = -\frac{3}{5}\overline{\frac{\partial u_k'}{\partial x_k}\delta_{ij}\frac{\partial u_i'}{\partial x_j}} - \frac{3}{5}\overline{\left(\frac{\partial u_i'}{\partial x_j} + \frac{\partial u_j'}{\partial x_i}\right)\frac{\partial u_i'}{\partial x_j}}$$

or

$$\frac{d^2\tilde{T}}{dy^2} - \frac{6(1-e)\tilde{T}}{\sigma^2} = -\frac{9}{5}\overline{\frac{\partial v'}{\partial y}\frac{\partial v'}{\partial y}}. \tag{51}$$

Using the expression (48) for v' in (51) we can solve for the mean granular temperature in the case of small attenuation:

$$\tilde{T} = A_{1,2}\, e^{\pm\beta^{\frac{1}{2}}y} + A\, e^{-2\delta y}, \tag{52}$$

where

$$\beta = 6(1-e)/\sigma^2, \tag{53}$$

$$A = \tfrac{9}{10} v_b^2 k^2/(\beta - 4\delta^2). \tag{54}$$

If we assume that the energy input occurs only at the bed and that (damped) waves travel in the positive y-direction, then $A_1 = 0$.

4.2. *Streaming motions*

Assuming that $\bar{\rho} \approx \rho_0$, the mean flow continuity equation (32) becomes

$$\frac{\partial \tilde{u}_i}{\partial x_i} = 0, \tag{55}$$

and the mean stress tensor (14) is approximately

$$\bar{p}_{ij} \approx \left[\bar{p}_{s_0} + \frac{\kappa}{\sigma}(\pi\tilde{T})^{\frac{1}{2}}\right]\delta_{ij} - \frac{3\kappa}{5}\left(\frac{\partial \tilde{u}_i}{\partial x_j} + \frac{\partial \tilde{u}_j}{\partial x_i}\right), \tag{56}$$

where, as noted previously, we have assumed that $\kappa \approx$ const.

The two-dimensional streaming flow patterns will be considered in a layer of granular material of small depth-to-width ratio; thus we define a small parameter

$$\epsilon = h/b \ll 1. \tag{57}$$

For simplicity we assume that the velocity of the base vibrations has the following explicit variation with x:

$$v_b(x) = v_0\left[1+\epsilon N\cos\left(\pi\frac{x}{b}\right)\right], \tag{58}$$

where $N = O(1)$.

Define dimensionless variables

$$\left.\begin{aligned} X=\frac{x}{b},\quad Y=\frac{y}{h},\quad U=\frac{\tilde{u}_1}{v_0\epsilon}=\frac{\tilde{u}}{v_0\epsilon},\quad V=\frac{\tilde{u}_2}{v_0\epsilon^2}=\frac{v}{v_0\epsilon^2},\\ P_s=\frac{p_{s_0}}{\rho_0 gh},\quad T_*^{\frac{1}{2}}=\frac{\kappa(\pi\tilde{T})^{\frac{1}{2}}}{\sigma\rho_0 gh},\end{aligned}\right\} \tag{59}$$

and put

$$\frac{6\kappa v_0}{5\rho_0 gh^2}=\mu\epsilon, \tag{60}$$

where $\mu = O(1)$.

Then the non-dimensional components of the stress tensor are

$$\left.\begin{aligned} P_{xx}&=\frac{p_{xx}}{\rho_0 gh}=P_s+T_*^{\frac{1}{2}}-\mu\epsilon^3\frac{\partial U}{\partial X},\\ P_{yy}&=\frac{p_{yy}}{\rho_0 gh}=P_s+T_*^{\frac{1}{2}}-\mu\epsilon^3\frac{\partial V}{\partial Y},\\ P_{yx}=P_{xy}&=\frac{p_{xy}}{\rho_0 gh}=-\tfrac{1}{2}\mu\epsilon^2\left[\frac{\partial U}{\partial Y}+\epsilon^2\frac{\partial V}{\partial X}\right].\end{aligned}\right\} \tag{61}$$

The dominant Reynolds stress $\overline{\rho u_i' u_j'}$ is

$$\overline{\rho u_2' u_2'} \approx \rho_0\overline{v'v'} = \rho_0\tfrac{1}{2}v_b^2\,e^{-2\delta y}. \tag{62}$$

With the above definitions, the mean continuity for steady streaming motions and the mean linear momentum equations in the x- and y-directions are respectively

$$\frac{\partial U}{\partial X}+\frac{\partial V}{\partial Y}=0, \tag{63}$$

$$\epsilon^2 M\left[U\frac{\partial U}{\partial X}+V\frac{\partial U}{\partial Y}\right]=-\frac{\partial}{\partial X}[P_s+T_*^{\frac{1}{2}}]+\epsilon^3\mu\frac{\partial^2 U}{\partial X^2}+\epsilon^{\frac{1}{2}}\mu\frac{\partial^2 U}{\partial Y^2}+\epsilon^{3\frac{1}{2}}\mu\frac{\partial^2 V}{\partial X\,\partial Y}, \tag{64}$$

$$\epsilon^4 M\left[U\frac{\partial V}{\partial X}+V\frac{\partial V}{\partial Y}\right]=-1+\tfrac{1}{2}\mu\epsilon^5\frac{\partial^2 V}{\partial X^2}+\tfrac{1}{2}\mu\epsilon^3\frac{\partial^2 V}{\partial Y^2}-\frac{\partial}{\partial Y}[P_s+T_*^{\frac{1}{2}}+\tfrac{1}{2}M\{1+\epsilon N\cos(\pi X)\}^2\,e^{-2\delta hY}], \tag{65}$$

where

$$M = v_0^2/gh = O(1). \tag{66}$$

Expanding the variables in powers of ϵ as

$$\begin{aligned} U&=U^{(0)}+\epsilon U^{(1)}+\epsilon^2 U^{(2)}+\ldots,\\ [P_s+T_*^{\frac{1}{2}}]&=[P_s+T_*^{\frac{1}{2}}]^{(0)}+\epsilon[P_s+T_*^{\frac{1}{2}}]^{(1)}+\ldots,\end{aligned} \tag{67}$$

etc., and substituting in (63), (64) and (65) we obtain the sequence of equations:

Zeroth-order

$$\frac{\partial U^{(0)}}{\partial X}+\frac{\partial V^{(0)}}{\partial Y}=0, \tag{68}$$

$$\frac{\partial}{\partial X}[P_s+T_*^{\frac{1}{2}}]^{(0)}=0, \tag{69}$$

$$\frac{\partial}{\partial Y}\{[P_s+T_*^{\frac{1}{2}}]^{(0)}+\tfrac{1}{2}M\,e^{-2\delta hY}\}=-1, \tag{70}$$

First-order

$$\frac{\partial}{\partial X}[P_s+T_*^{\frac{1}{2}}]^{(1)}=\tfrac{1}{2}\mu\frac{\partial^2 U^{(0)}}{\partial Y^2}, \tag{71}$$

$$\frac{\partial}{\partial Y}\{[P_s+T_*^{\frac{1}{2}}]^{(1)}+MN\cos(\pi X)\,e^{-2\delta hY}\}=0 \tag{72}$$

etc.

Solution of the above equations is sufficient to reveal the main features of the streaming flow. Integrating (69) and (70) and taking the normal stress to be zero at the free surface $Y=1$ yields

$$[P_s+T_*^{\frac{1}{2}}]^{(0)}=1-Y+\tfrac{1}{2}M[e^{-2\delta h}-e^{-2\delta hY}]. \tag{73}$$

Integrating (72) and again applying the condition that the normal stress is zero at the free surface yields

$$[P_s+T_*^{\frac{1}{2}}]^{(1)}=-MN\cos(\pi X)[e^{-2\delta hY}-e^{-2\delta h}]. \tag{74}$$

By substituting (74) in (71) and integrating once we find

$$\tfrac{1}{2}\mu\frac{\partial U^{(0)}}{\partial Y}=-\pi MN\sin(\pi X)\left[\frac{1}{2\delta h}e^{-2\delta hY}+Y\,e^{-2h\delta}\right]+G_1(X). \tag{75}$$

At the upper free 'surface' one can observe a cloud of saltating particles or a 'boundary layer' in which the bulk density gradually varies from its value in the interior of the bed to zero. Thus, although the shear stress is zero along the upper 'surface', the bulk density, κ and μ also are zero there and the application of the stress-free condition for the determination of $G_1(X)$ is awkward. Instead we apply an approximate condition at the base $Y=0$ where properties are better defined. It is assumed that the base is smooth, particles slip, and that the shear stress and thus $\partial U^{(0)}/\partial Y$ are zero there. Thus we find

$$G_1(X)=\frac{\pi MN}{2\delta h}\sin(\pi X). \tag{76}$$

Integrating (75) again yields

$$\tfrac{1}{2}\mu U^{(0)}=\pi MN\sin(\pi X)\left\{\frac{1}{2\delta h}\left[Y+\frac{e^{-2\delta hY}}{2\delta h}\right]-\tfrac{1}{2}Y^2\,e^{-2\delta h}\right\}+G_2(X). \tag{77}$$

Since the streaming flows have the form of recirculating gyres, we can determine $G_2(X)$ by using the condition that

$$\int_0^1 U^{(0)}\,dY=0. \tag{78}$$

Hence we find that

$$G_2(X) = \pi MN \sin(\pi X)\left\{\tfrac{1}{6}\,\mathrm{e}^{-2\delta h} + \frac{1}{8\delta^3 h^3}[\mathrm{e}^{-2\delta h} - 1] - \frac{1}{4\delta h}\right\}. \tag{79}$$

Integrating the continuity equation (68) using (77) and (79) yields the zeroth-order vertical velocity component

$$V^{(0)} = -\frac{2\pi^2 MN}{\mu}\cos(\pi X)\left\{\frac{1}{2\delta h}\left[\tfrac{1}{2}Y^2 + \frac{1}{4\delta^2 h^2} - \frac{\mathrm{e}^{-2\delta h Y}}{4\delta^2 h^2}\right]\right.$$
$$\left. -\tfrac{1}{6}Y^3\,\mathrm{e}^{-2\delta h} + Y\left[\tfrac{1}{6}\,\mathrm{e}^{-2\delta h} - \frac{1}{4\delta h} + \frac{1}{8\delta^3 h^3}(\mathrm{e}^{-2\delta h} - 1)\right]\right\}. \tag{80}$$

5. Comparison of predicted streaming flow velocities with measurements

It is interesting to compare the predicted zeroth-order streaming velocities with the experimental data shown in figure 3. Most of the values for material properties and granular-bed dimensions required for the calculations were determined in the experiments, but some other quantities must be estimated. Furthermore, to simplify the calculations we shall make use of overall average values for κ, ρ_0, μ, δ, etc.

Equation (52) gives the mean granular temperature distribution. If we assumed, for example, that to first order all the normal stresses at the base arise from collisional interactions, then from (73) applied at $Y = 0$ we obtain

$$T_*^{\frac{1}{2}} \approx 1. \tag{81}$$

Hence from (8) and (59), at $Y = 0$ we find

$$\tilde{T} \approx \frac{gh}{2(1+e)\,\nu g_0(\nu)}. \tag{82}$$

Equating (82) to (52) applied at $y = 0$ provides a means to determine the constant A_2 and hence the resulting granular temperature distribution as a function of distance above the base. For typical plastic and glass particles $e \approx 0.8$–0.95 (Lun & Savage 1986). Thus $\beta^{-\frac{1}{2}}$ is of the order of a particle diameter σ and it will be found that $\delta^2 \ll \beta$. The e-folding distance for the first term on the right-hand side of (52) is of the order of one particle diameter. Hence the temperature distribution $\tilde{T}$ over almost the entire depth is dominated by the second term $A\exp(-2\delta y)$ which decays slowly with y since δ is very small. Thus one finds a thin layer near the vibrating bed where the granular temperature is highest at the very bottom and drops off very rapidly with height. In the main part of the interior the granular temperature $\tilde{T}$ is lower and nearly constant, and ν is somewhat larger than in the thin high-granular-temperature bed layer. We shall assume an overall average value of $\nu = 0.58$, $e = 0.85$ and estimate an overall average granular temperature to be used in the determination of the average values for κ, ρ_0, μ, δ, etc. The average particle diameter is chosen as $\sigma = \frac{1}{2}(0.8+2.0) = 1.4$ mm. We also take $\epsilon N = 0.5$. This will closely approximate the base vibration amplitude over most of the bed, but it gives values that are too high near the sidewalls ($X = \pm 1$) and will probably cause the predictions to overestimate the streaming velocities.

Since the high-temperature layer next to the vibrating plate is very thin and δ is very small, a good approximation to the overall average temperature is seen from (52) to be

$$\tilde{T} \approx A. \tag{83}$$

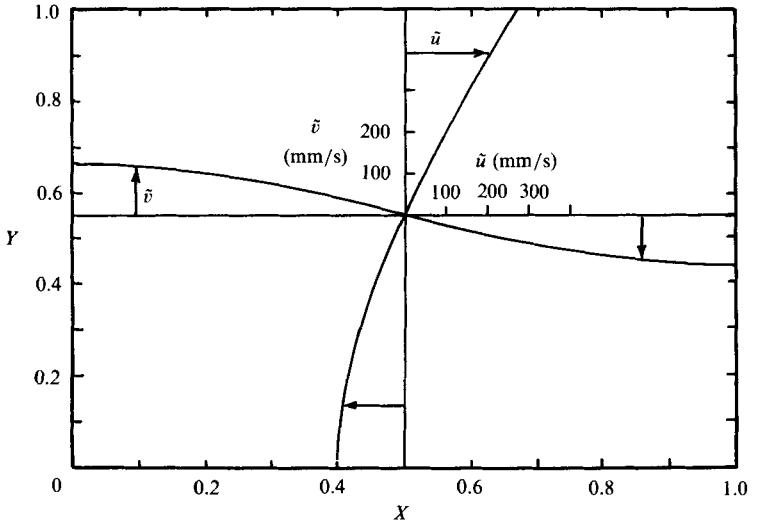

FIGURE 5. Horizontal and vertical components of streaming velocities on vertical and horizontal lines respectively through the centre of the right-hand gyre (for $a = 3$ mm, $f = 25$ Hz, $e = 0.85$ and average $h = 62$ mm).

Taking $\delta^2 \ll \beta$ in (54), and using (19), (8), (49) and (60) it is possible to calculate the overall average temperature and c_0, κ, δ and μ corresponding to this overall average granular temperature. We can then determine the streaming velocity components from (77) and (78).

Figure 5 shows the predicted u- and v-velocity components along vertical and horizontal lines respectively passing through the centre of the right-hand gyre. The velocities were calculated for base vibration centreline amplitude $a = v_0(1+\epsilon N)/\omega = 3$ mm, a frequency of 25 Hz, a coefficient of restitution $e = 0.85$ and an average depth of material $h = 62$ mm. The flow pattern is similar to that observed but the predicted magnitude of the velocities is about an order of magnitude too large.

Figure 6 shows the magnitude of the predicted velocity V_P at the point P ($x = 24$ mm, $y = 32$ mm) versus base vibration frequency f for constant values of bed centreline vibration amplitude a. The streaming velocities increase with increasing a and depend linearly upon vibration frequency.

The predicted velocities are considerably higher than the experimental measurements shown in figure 3. This is to be expected since we have made several simplifying assumptions in the analysis which result in overestimates of the streaming velocities. The friction along the front, back and sidewalls and base has been neglected; and the static contribution to the *shear stress* has been neglected in the interior of the granular material (recall φ was assumed zero in (12)). In the experimental set-up the amplitude of the base vibration decreased to approximately zero at the sidewalls ($X = \pm 1$). Thus near these walls the granular material would not be fluidized to the same extent as material closer to the centreline, the internal friction and 'viscosity' would be high and the circulation velocities reduced as a result.

It may also be noted that the predicted velocity versus frequency curves of figure 6 have a different shape than the experimental curves of figure 3. At high frequencies and high base vibration amplitudes a new phenomenon enters. It has been neglected in the analysis and it is difficult to see how it might be incorporated. If the velocity

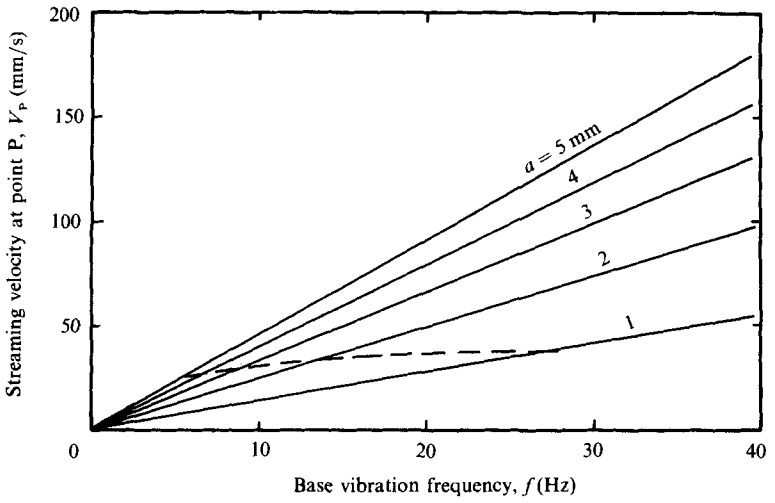

FIGURE 6. Predicted magnitude of streaming velocity at point P as a function of bed vibration frequency and amplitude for $e = 0.85$. Results above the dashed line, which corresponds to $v_0 = \langle C^2 \rangle^{\frac{1}{2}}$, would be affected by loss of contact of the granular bed with the vibrating bottom.

of the base vibrations is too high, the base will lose collisional contact with the particles over a portion of each cycle. This kind of 'chattering' was observed in the experiments at high frequencies and amplitudes.

We can roughly estimate the frequency at which the base *begins* to lose collisional contact by putting the mean base velocity v_0 equal to the r.m.s. of the individual particle velocity fluctuations, i.e.

$$v_0 = \langle C^2 \rangle^{\frac{1}{2}} = (3T)^{\frac{1}{2}}; \tag{84}$$

hence we find

$$f = \frac{(1+\epsilon N)}{2\pi a}(3T)^{\frac{1}{2}}. \tag{85}$$

A line corresponding to (84) is plotted on figure 6; the region above this line will be affected by loss of base contact with the particles. As a result of this 'chattering', the vibrating bottom is less effective in generating waves that fluidize the granular material. The streaming velocities would be less than those shown in figure 6, and would tend to zero for large bottom vibration amplitude and frequency rather than increasing monotonically as predicted.

6. Concluding remarks

The slow streaming motions developed in a bed of dry granular material fluidized by a vibrating bottom have been studied both experimentally and theoretically. Heretofore, no convincing explanation for these flows has been given. The present paper has proposed that they are analogous to the phenomenon of 'acoustic streaming', and a simple analysis of the streaming motion was given. The acoustic streaming referred to here results from dissipation in the interior of the granular material and is not the boundary-layer type of streaming responsible for the collection of lycopodium powder on vibrating plates. The approximate theory yields the general qualitative features of the flow patterns, but it overestimates the magnitude of the streaming velocities. This was anticipated because of the numerous

simplifying assumptions that were necessary to enable a simple closed-form solution. However, the main purpose of the analysis was to identify and corroborate the mechanisms responsible for the streaming motions and this appears to have been accomplished.

While under certain conditions the non-uniform base vibrations are effective in mixing the granular materials, the functioning of this mechanism is limited to rather small depths of material, of the order of 10 cm for typical plastic or glass particles of millimeter size. It may be worthwhile to investigate mixing in a bed using the combination of usual gas or liquid fluidization with the vibrational fluidization described in the present paper.

Grateful acknowledgement is made to the Natural Sciences and Engineering Research Council of Canada for support of this work.

REFERENCES

BAGNOLD, R. A. 1954 Experiments on a gravity-free dispersion of large solid spheres in a Newtonian fluid under shear. *Proc. R. Soc. Lond.* A **225**, 49–63.

CAMPBELL, C. S. & BRENNEN, C. E. 1983 Computer simulation of shear flows of granular material. In *Mechanics of Granular Materials: New Models and Constitutive Relations* (ed. J. T. Jenkins & M. Satake), pp. 313–326. Elsevier.

CAMPBELL, C. S. & BRENNEN, C. E. 1985 Chute flows of granular material: some computer simulations. *Trans. ASME* E: *J. Appl. Mech.* **52**, 172–178.

CARNAHAN, N. F. & STARLING, K. E. 1969 Equations of state for non-attracting rigid spheres. *J. Chem. Phys.* **51**, 635–636.

CEBECI, T. & SMITH, A. M. O. 1974 *Analysis of Turbulent Boundary Layers.* Academic.

CHAPMAN, S. & COWLING, T. G. 1960 *The Mathematical Theory of Non-Uniform Gases*, 2nd edn. Cambridge University Press.

FARADAY, M. 1831 On a peculiar class of acoustical figures assumed by groups of particles upon vibrating elastic surfaces. *Phil. Trans. R. Soc. Lond.* 299–340 (see also *Faraday's Diary*, Vol. 1 (ed. T. Martin), pp. 324–359. G. Bell & Sons Ltd., London.)

GUTMAN, R. G. 1976 Vibrated beds of powders. Part 1. A theoretical model for the vibrated bed. *Trans. Inst. Chem. Engrs* **54**, 174–183.

HAFF, P. K. 1983 Grain flow as a fluid-mechanical phenomenon. *J. Fluid Mech.* **134**, 401–430.

JENKINS, J. T. & RICHMAN, M. W. 1985 Grad's 13-moment system for a dense gas of inelastic spheres. *Arch. Rat. Mech. Anal.* **87**, 355–377.

JENKINS, J. T. & SAVAGE, S. B. 1983 A theory for the rapid flow of identical, smooth, nearly elastic, spherical particles. *J. Fluid Mech.* **130**, 187–202.

KROLL, W. 1955 Fliesserscheinungen an Haufwerken in schwingenden Gafassen. *Chem. Ingr.-Tech.* **27**, 33.

LIGHTHILL, J. 1978 *Waves in Fluids.* Cambridge University Press.

LUN, C. K. K. & SAVAGE, S. B. 1986 The effects of an impact velocity dependent coefficient of restitution on stresses developed by sheared granular materials. *Acta Mech.* **63**, 15–44.

LUN, C. K. K., SAVAGE, S. B., JEFFREY, D. J. & CHEPURNIY, N. 1984 Kinetic theories for granular flow: inelastic particles in Couette flow and slightly inelastic particles in a general flow field. *J. Fluid Mech.* **140**, 223–256.

OGAWA, S., UMEMURA, A. & OSHIMA, N. 1980 On the equations of fully fluidized granular materials. *Z. Angew. Math. Phys.* **31**, 483–493.

RÁTKAI, G. 1976 Particle flow and mixing in vertically vibrated beds. *Powder Technol.* **15**, 187–192.

SAVAGE, S. B. 1983*a* Granular flows at high shear rates. In *Theory of Dispersed Multiphase Flow* (ed. R. E. Meyer), pp. 339–358. Academic.

SAVAGE, S. B. 1983*b* Granular flows down rough inclines: Review and extension. In *Mechanics of*

Granular Materials: New Models and Constitutive Relations (ed. J. T. Jenkins & M. Satake), pp. 261–282. Elsevier.

SAVAGE, S. B. 1984 The mechanics of rapid granular flows. In *Advances in Applied Mechanics*, vol. 24 (ed. J. Hutchinson & T. Y. Wu), pp. 289–366. Academic.

SAVAGE, S. B. & JEFFREY, D. J. 1981 The stress tensor in a granular flow at high shear rates. *J. Fluid Mech.* **110**, 225–272.

SAVAGE, S. B. & SAYED, M. 1984 Stresses developed by dry cohesionless granular materials sheared in an annular shear cell. *J. Fluid Mech.* **142**, 391–430.

SHEN, H. & ACKERMANN, N. L. 1982 Constitutive relationships for fluid-solid mixtures. *J. Engng Mech. Div. ASCE* **108**, 748–763.

SUZUKI, A., TAKAHASHI, H. & TANAKA, T. 1968/9 Behaviour of a particle bed in a field of vibration. III. Mixing of particles in a vibrating bed. *Powder Technol.* **2**, 78–81.

TAKAHASHI, H., SUZUKI, A. & TANAKA, T. 1968/9 Behaviour of a particle bed in a field of vibration. I. Analysis of particle motion in a vibrating vessel. *Powder Technol.* **2**, 65–71.

WALKER, J. 1982 The amateur scientist. *Scient. Am.* **247**, 206–216.